

# Exploring the Function Space of Deep-Learning Machines

Bo Li<sup>1,\*</sup> and David Saad<sup>2,†</sup>

<sup>1</sup>*Department of Physics, The Hong Kong University of Science and Technology, Hong Kong*

<sup>2</sup>*Non-linearity and Complexity Research Group, Aston University, Birmingham B4 7ET, United Kingdom*

The function space of deep-learning machines is investigated by studying growth in the entropy of functions of a given error with respect to a reference function, realized by a deep-learning machine. Using physics-inspired methods we study both sparsely and densely-connected architectures to discover a layer-wise convergence of candidate functions, marked by a corresponding reduction in entropy when approaching the reference function, gain insight into the importance of having a large number of layers, and observe phase transitions as the error increases.

Deep-learning machines (DLM) have both fascinated and bewildered the scientific community and have given rise to an active and ongoing debate [1]. They are carefully structured layered networks of non-linear elements, trained on data to perform complex tasks such as speech recognition, image classification, and natural language processing. While their phenomenal engineering successes [2] have been broadly recognized, their scientific foundations remain poorly understood, particularly their good ability to generalize well from a limited number of examples with respect to the degrees of freedom and the nature of the layer-wise internal representations.

The parameter estimation in DLM, termed supervised learning, is based on the introduction of example pairs of input and output patterns, which serve as constraints on space of candidate functions. As more examples are introduced the function space monotonically decreases. Statistical physics methods have been successful in gaining insight into both pattern-storage [3] and learning scenarios, mostly in single layer machines [4] but also in simple two-layer scenarios [5, 6]. However, extending these methods to DLM is difficult due to the recursive application of non-linear functions in successive layers and the undetermined degrees of freedom in intermediate layers. While training examples determine both input and output patterns, the constraint imposed on hidden-layer representations are difficult to pin down. These constitute the main difficulties for a better understanding of DLM.

In this Letter, we propose a general framework for analyzing DLM by mapping them onto a dynamical system and by employing the Generating Functional (GF) approach to analyze their typical behavior. More specifically, we investigate the landscape in function space around a reference function by perturbing its parameters (weights in the DLM setting), and quantifying the entropy of the corresponding functions space for a given level of error with respect to the reference function. Such setup is reminiscent of the teacher-student scenario, commonly used in the neural networks literature [7] where the average error serves as a measure of distance between the perturbed and reference network in function space. For certain classes of reference networks, we obtain closed form solutions of the error as a function of

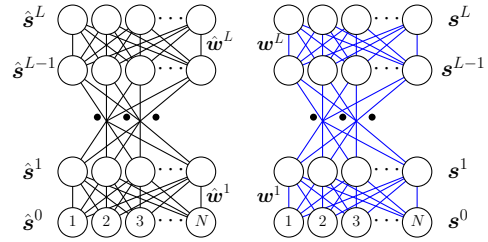


Figure 1. (Color online). The model of two coupled DLMs. The reference and perturbed functions are denoted by  $\{\hat{w}^l\}$  (black edges) and  $\{w^l\}$  (blue edges), respectively.

perturbation on each layer, and consequently the phase volume for a given level of function error. By the virtue of supervised learning and constraints imposed by the examples provided, high-error functions will be ruled out faster than those with low errors, such that the candidate function space is reduced and the concentration of low-error functions increases. A somewhat similar approach, albeit based on recursive mean field relations between each two consecutive layers separately, has been used to probe the expressivity of DLM [8].

Through the GF framework and entropy maximization, we analyze the typical behavior of different classes of models including networks with continuous and binary parameters (weights) and different topologies, both fully and sparsely connected. We find that as one lowers the error level, typical functions gradually better match the reference network *starting from earlier layers to later ones*. More drastically, for fully connected binary networks, weights in earlier layers of the perturbed functions will perfectly match those of the reference function, implying a possible successive layer by layer learning behavior. Sparsely connected topologies exhibit phase transitions with respect to the number of layers, by varying the magnitude of perturbation, similar to the phase transitions in noisy Boolean computation [9], which support the need of deep networks for improving generalization.

*Densely connected network models.*—The model considered here comprises two coupled feed-forward DLM as illustrated in Fig. 1, one of which serves as the ref-

erence function and the other is obtained by perturbing the reference network parameters. We first consider the densely connected networks. Each network is composed of  $L+1$  layers of  $N$  neurons each. The reference function is parameterized by  $N^2 \times L$  weight variables  $\hat{w}_{ij}^l, \forall l = 1, 2, \dots, L, i, j = 1, 2, \dots, N$  and maps an  $N$ -dimensional input  $\hat{\mathbf{s}}^0 \in \{-1, 1\}^N$  to an  $N$ -dimensional output  $\hat{\mathbf{s}}^L \in \{-1, 1\}^N$ , through intermediate-layer internal representations and according to the stochastic rule

$$P(\hat{\mathbf{s}}^L | \hat{\mathbf{w}}, \hat{\mathbf{s}}^0) = \prod_{l=1}^L P(\hat{\mathbf{s}}^l | \hat{\mathbf{w}}^l, \hat{\mathbf{s}}^{l-1}). \quad (1)$$

The  $i$ -th neuron in the  $l$ -th layer experiences a local field  $\hat{h}_i^l(\hat{\mathbf{w}}^l, \hat{\mathbf{s}}^{l-1}) = \frac{1}{\sqrt{N}} \sum_j \hat{w}_{ij}^l \hat{s}_j^{l-1}$ , and its state is determined by the conditional probability

$$P(\hat{s}_i^l | \hat{\mathbf{w}}^l, \hat{\mathbf{s}}^{l-1}) = \frac{e^{\beta \hat{s}_i^l \hat{h}_i^l(\hat{\mathbf{w}}^l, \hat{\mathbf{s}}^{l-1})}}{2 \cosh \left[ \beta \hat{h}_i^l(\hat{\mathbf{w}}^l, \hat{\mathbf{s}}^{l-1}) \right]}, \quad (2)$$

where the temperature  $\beta$  quantifies the strength of thermal noise. In the noiseless limit  $\beta \rightarrow \infty$ , node  $i$  represents a perceptron  $\hat{s}_i^l = \text{sgn}(\hat{h}_i^l)$  and Eq. (1) corresponds to a deterministic neural network with a *sign* activation function. The perturbed network operates in the same manner, but the weights  $w_{ij}^l$  are obtained by applying independent perturbation to each of the reference weights; the perturbed weights  $\hat{w}_{ij}^l$ , give rise to a function that is correlated with the reference function.

We focus on the similarity between reference and perturbed functions outputs for randomly sampled input patterns  $\mathbf{s}^0 = \hat{\mathbf{s}}^0$ , drawn from some distribution  $P(\hat{\mathbf{s}}^0)$ . Considering the joint probability of the two systems

$$P[\{\hat{\mathbf{s}}^l\}, \{\mathbf{s}^l\}] = P(\hat{\mathbf{s}}^0) \prod_{i=1}^N \delta_{\hat{s}_i^0, \mathbf{s}_i^0} \prod_{l=1}^L P(\hat{\mathbf{s}}^l | \hat{\mathbf{w}}^l, \hat{\mathbf{s}}^{l-1}) P(\mathbf{s}^l | \mathbf{w}^l, \mathbf{s}^{l-1}), \quad (3)$$

where the weight parameters  $\{\hat{w}_{ij}^l\}$  and  $\{w_{ij}^l\}$  are quenched disordered variables. We consider two cases, where the weights are continuous or discrete variables drawn from the Gaussian and Bernoulli distributions, respectively. The quantity of interests are the overlaps between the two functions at the different layers  $q^l(\hat{\mathbf{w}}, \mathbf{w}) \equiv \frac{1}{N} \sum_i \langle \hat{s}_i^l \mathbf{s}_i^l \rangle$ , where angled brackets  $\langle \dots \rangle$  denote the average over the joint probability  $P[\{\hat{\mathbf{s}}^l\}, \{\mathbf{s}^l\}]$ . The  $N$  outputs represent  $N$  weakly coupled Boolean functions of the same form of disordered, and thus share the same average behavior.

The form of probability distribution (3) is analogous to the dynamical evolution of disordered Ising spin systems [10] if the layers are viewed as discrete time steps of parallel dynamics. We therefore apply the GF formulation from statistical physics to these deep feed-forward functions similarly to the approach

used to investigate random Boolean formulae [9]. We compute the GF  $\Gamma[\hat{\boldsymbol{\psi}}, \boldsymbol{\psi}] = \left\langle e^{-i \sum_{l,i} (\hat{\psi}_i^l \hat{s}_i^l + \psi_i^l \mathbf{s}_i^l)} \right\rangle$ , from which the moments can be calculated, e.g.,  $q^l(\hat{\mathbf{w}}, \mathbf{w}) = -\frac{1}{N} \sum_i \lim_{\hat{\boldsymbol{\psi}}, \boldsymbol{\psi} \rightarrow 0} \frac{\partial^2}{\partial \hat{\psi}_i^l \partial \psi_i^l} \Gamma[\hat{\boldsymbol{\psi}}, \boldsymbol{\psi}]$ . Assuming the systems are self-averaging for  $N \rightarrow \infty$  and computing the disorder average (denoted by the upper line)  $\overline{\Gamma[\hat{\boldsymbol{\psi}}, \boldsymbol{\psi}]}$ , the disorder-averaged overlaps can be obtained  $q^l = \frac{1}{N} \sum_{i=1}^N \langle \hat{s}_i^l \mathbf{s}_i^l \rangle$ . For convenience, we introduce the field doublet  $H^l \equiv [\hat{h}^l, h^l]^T$ . Expressing the GF  $\Gamma[\hat{\boldsymbol{\psi}}, \boldsymbol{\psi}]$  by macroscopic order parameters and averaging over the disorder yields the saddle-point integral  $\overline{\Gamma} = \int \{d\mathbf{q}d\mathbf{Q}\} e^{N\Psi[\mathbf{q}, \mathbf{Q}]}$  where  $\Psi[\dots]$  is [11]

$$\Psi = i \sum_{l=0}^L \mathcal{Q}^l q^l + \log \int \prod_{l=1}^L d\hat{h}^l dh^l \sum_{\{\hat{s}^l, \mathbf{s}^l\}} M[\hat{s}, s, \hat{h}, h], \quad (4)$$

and the effective single site measure  $M[\dots]$  has the following form for both continuous and binary weights

$$M[\hat{s}, s, \hat{h}, h] = P(\hat{s}^0) \delta_{\hat{s}^0, \mathbf{s}^0} e^{-i \sum_{l=0}^L \mathcal{Q}^l \hat{s}^l \mathbf{s}^l} \times \prod_{l=1}^L \left\{ \frac{e^{\beta \hat{s}^l \hat{h}^l}}{2 \cosh \beta \hat{h}^l} \frac{e^{\beta \mathbf{s}^l h^l}}{2 \cosh \beta h^l} \frac{e^{-\frac{1}{2} (H^l)^T \cdot \Sigma_l^{-1} \cdot H^l}}{\sqrt{(2\pi)^2 |\Sigma_l(q^{l-1})|}} \right\}. \quad (5)$$

The Gaussian density of the local field  $\{\hat{h}^l, h^l\}$  in (5) comes from summing a large number of random variables in  $\hat{h}^l$  and  $h^l$ . The precision matrix  $\Sigma_l^{-1}$ , linking the effective field  $\hat{h}^l$  and  $h^l$ , measures the correlation between internal fields of the two systems and depends on the overlap  $q^{l-1}$  of the previous layer. In the limit  $N \rightarrow \infty$  the GF  $\overline{\Gamma}$  is dominated by the extremum of  $\Psi$ . Variation with respect to  $\mathcal{Q}^l$  gives rise to saddle-point equations of the order parameters  $q^l = \langle \hat{s}^l \mathbf{s}^l \rangle_{M[\dots]}$ , where the average is taken over the measure  $M[\dots]$  of (5). The conjugate order parameter  $\mathcal{Q}^l$ , ensuring the normalization of the measure, vanishes identically. It leads to the evolution equation [11]

$$q^l = \int d\hat{h}^l dh^l \tanh(\beta \hat{h}^l) \tanh(\beta h^l) \frac{e^{-\frac{1}{2} (H^l)^T \cdot \Sigma_l^{-1} \cdot H^l}}{\sqrt{(2\pi)^2 |\Sigma_l|}}. \quad (6)$$

*Densely connected continuous weights*—In the first scenario, we assume weight variables  $\hat{w}_{ij}^l$  to be independently drawn from a Gaussian density  $\mathcal{N}(0, \sigma^2)$  and the perturbed weights to have the form  $w_{ij}^l = \sqrt{1 - (\eta^l)^2} \hat{w}_{ij}^l + \eta^l \delta w_{ij}^l$ , where  $\delta w_{ij}^l$  are drawn from  $\mathcal{N}(0, \sigma^2)$  independently of  $\hat{w}_{ij}^l$ . It ensures that  $w_{ij}^l$  has the same variance  $\sigma^2$ . The parameter  $\eta^l$  quantifies the strength of perturbation introduced in layer  $l$ . In this case the correlation matrix between the local fields  $\hat{h}^l$  and  $h^l$  takes the form

$$\Sigma_l(\eta^l, q^{l-1}) = \sigma^2 \begin{bmatrix} 1 & \sqrt{1 - (\eta^l)^2} q^{l-1} \\ \sqrt{1 - (\eta^l)^2} q^{l-1} & 1 \end{bmatrix}, \quad (7)$$

leading to the close form solution of the overlap as  $\beta \rightarrow \infty$ ,

$$q^l = \frac{2}{\pi} \sin^{-1} \left( \sqrt{1 - (\eta^l)^2 q^{l-1}} \right). \quad (8)$$

Of particular interest is the final-layer overlap given the same input for the two system under specific perturbations  $q^L(\{\eta^l\}, q^0 = 1)$ . The average error  $\varepsilon = \frac{1}{2}(1 - q^L)$  measures the typical distance between the two mappings.

The number of solutions at a given distance (error)  $\varepsilon$  away from the reference function is indicative of how difficult it is to obtain this level of approximation at the vicinity of the exact function. Let the  $N$ -dimensional vectors  $\hat{w}^{l,i}$  and  $w^{l,i}$  denote the weights of the  $i$ -th perceptron of the reference and perturbed systems at layer  $l$ , respectively; the expected angle between them is  $\theta^l = \sin^{-1} \eta^l$ . Then the perceptron  $w^{l,i}$  occupies on average an angular volume around  $w^{l,i}$  as  $\Omega(\eta^l) \sim \sin^{N-2} \theta^l = (\eta^l)^{N-2}$  [12, 13]. The total phase volume of the perturbed system is  $\Omega_{\text{tot}}(\{\eta^l\}) = \prod_{l=1}^L \prod_i (\eta^l)^{N-2}$ , and the corresponding entropy density is

$$S_{\text{con}}(\{\eta^l\}) = \frac{1}{LN^2} \log \Omega_{\text{tot}}(\{\eta^l\}) \approx \frac{1}{L} \sum_{l=1}^L \log \eta^l. \quad (9)$$

In the thermodynamic limit  $N \rightarrow \infty$ , the set of perturbed functions at distance  $\varepsilon$  away from the reference function is dominated by those with perturbation vector  $\{\eta^{*l}\}$ , which maximizes the entropy  $S_{\text{con}}(\{\eta^l\})$  subject to the constraint  $q^L(\{\eta^l\}) = 1 - 2\varepsilon$ . The result of  $\{\eta^{*l}\}$  for a four-layer network, shown in Fig. 2(a), reveals that the dominant perturbation  $\eta^{*l}$  to the reference network decays faster for smaller  $l$  values; this indicates that closer to the reference function, solutions are dominated by functions where early-layer weights match better the reference network. Consequently, high- $\varepsilon$  function are ruled out faster during training through the successful alignment of earlier layers, resulting in the increasing concentration of low- $\varepsilon$  functions and better generalization.

Supervised learning is based on the introduction of input-output example pairs. Introducing constraints, in the form of  $P \equiv \alpha LN^2$  examples provided by the reference function, the phase volume at small distance  $\varepsilon$  away from the reference function is re-shaped as  $\Omega_\alpha(\varepsilon) = \Omega_{\text{tot}}(\{\eta^{*l}\}, \varepsilon)(1 - \varepsilon)^P$  in the annealed approximation [12, 13]; details of the derivation can be found in [11]. The typical distance  $\varepsilon^*(\alpha) = \text{argmax}_\varepsilon \Omega_\alpha(\varepsilon)$  can be interpreted as the generalization error in the presence of  $P$  examples, giving rise to an approximated generalization curves shown in Fig. 2(c). It is observed that typically a large number of examples ( $\alpha \gg 10$ ) are needed for good generalization. This may imply that DLMs trained on realistic data sets (usually  $\alpha \ll 1$ ) occupy a small, highly-biased subspace, different from the typical function space analyzed here (e.g., the handwritten digit NIST database represents highly biased inputs that occupy a very small fraction of the input space).

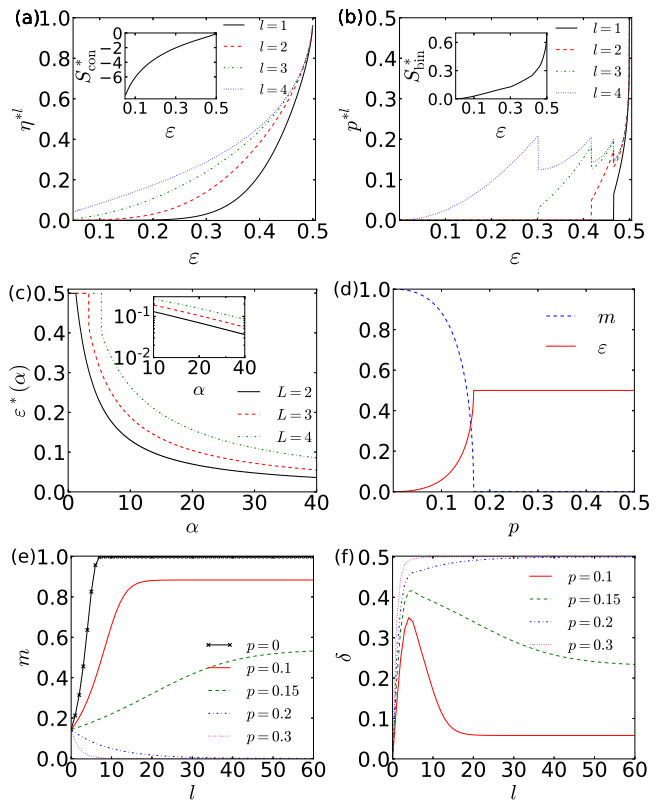


Figure 2. (Color online) Maximal-entropy perturbations as a function of output error  $\varepsilon$  for a four-layer densely-connected networks with (a) continuous weights and (b) binary weights. Inset represents the growth in entropy with respect to  $\varepsilon$ . (c) Generalization curves of densely-connected networks with continuous weights by using the annealed approximation. Inset demonstrates the classical asymptotic behavior of  $\varepsilon^* \sim \alpha^{-1}$  in the large  $\alpha$  limit [13]. (d) Stationary magnetization  $m$  and function error  $\varepsilon$  for sparsely connected MAJ-3 based DLM as a function of perturbation probability  $p$  in networks with binary weights. We show the evolution of (e) magnetization and (f) internal activation error  $\delta$  over layers. Note that  $p=0$  corresponds to the reference network.

*Densely connected binary weights*—Next we consider a reference network with binary weight variables drawn from the distribution  $P(\hat{w}_{ij}^l) = \frac{1}{2}\delta_{\hat{w}_{ij}^l, 1} + \frac{1}{2}\delta_{\hat{w}_{ij}^l, -1}$ , while the perturbed network weights follow the distribution  $P(w_{ij}^l) = (1 - p^l)\delta_{w_{ij}^l, \hat{w}_{ij}^l} + p^l\delta_{w_{ij}^l, -\hat{w}_{ij}^l}$ , where  $p^l$  is the flipping probability at layer  $l$ . The correlation matrix

$$\Sigma_l(p^l, q^{l-1}) = \begin{bmatrix} 1 & (1 - 2p^l)q^{l-1} \\ (1 - 2p^l)q^{l-1} & 1 \end{bmatrix}, \quad (10)$$

gives rise to overlaps  $q^l$  as  $\beta \rightarrow \infty$  of the form

$$q^l = \frac{2}{\pi} \sin^{-1} \left( (1 - 2p^l)q^{l-1} \right). \quad (11)$$

The entropy density of the perturbed system is given by

$$S_{\text{bin}}(\{p^l\}) = \frac{1}{L} \sum_{l=1}^L -p^l \log p^l - (1 - p^l) \log(1 - p^l). \quad (12)$$

Similarly, the entropy  $S_{\text{bin}}(\{p^l\})$  is maximized by the perturbation vector  $\{p^{*l}\}$  subject to  $q^L(\{p^l\}) = 1 - 2\varepsilon$  at a distance  $\varepsilon$  away from the reference function. The result of  $\{p^{*l}\}$  for a four-layer binary neural network is shown in Fig. 2(b). Surprisingly, as  $\varepsilon$  decreases, the first-layer weights are first to align perfectly with those of the reference function followed by the second-layer weights and so on. The discontinuities come from the non-convex nature of the entropy landscape  $S_{\text{bin}}(\{p^l\})$  when one restricts the perturbed system to the nonlinear  $\varepsilon$ -error surface satisfying  $q^L(\{p^l\}) = 1 - 2\varepsilon$ . Nevertheless, there exists many more high- $\varepsilon$  than low- $\varepsilon$  functions for densely-connected binary networks (as indicated by the entropy shown in the inset of Fig. 2(b)), and it remains to explore how low generalization error functions could be identified.

*Sparingly connected binary weights*—Lastly, we consider the sparsely connected DLM with binary weights. The layered setup is similar to the previous case, except that unit  $i$  at layer  $l$  is randomly connected to a small number  $k$  of units in layer  $(l-1)$  and its local field is given by  $\hat{h}_i^l(\hat{\mathbf{w}}^l, \hat{\mathbf{s}}^{l-1}) = \frac{1}{\sqrt{k}} \sum_j A_{ij}^l \hat{w}_{ij}^l \hat{s}_j^{l-1}$  where the adjacency matrix  $A^l$  represents the connectivity between the two layers. The perturbed network has the same topology but its weights are randomly flipped  $P(w_{ij}^l) = (1-p^l)\delta_{w_{ij}^l, \hat{w}_{ij}^l} + p^l\delta_{w_{ij}^l, -\hat{w}_{ij}^l}$ ; the activation and the joint probability of the two systems follow from (2) and (3). Unlike the case of densely-connected networks, the magnetization  $m^l \equiv \frac{1}{N} \sum_i s_i^l$  also plays an important role in the evolution of sparse networks. The GF approach gives rise to the order parameter  $\mathcal{P}^l(\hat{s}, s) \equiv \frac{1}{N} \sum_i \delta_{\hat{s}_i^l, s} \delta_{s_i^l, s}$  relating to the magnetization and overlap by  $\mathcal{P}^l(\hat{s}, s) = \frac{1}{4}(1 + \hat{s}m^l + sm^l + \hat{s}sq^l)$ .

The random topology provides an additional disorder to average over. For simplicity, we assign the reference weights to  $\hat{w}_{ij}^l = 1$ , which in the limit  $\beta \rightarrow \infty$  relate to the  $k$ -majority gate (MAJ- $k$ ) based Boolean formulas that provide all Boolean functions with uniform probability at the large  $L$  limit [14, 15]. For a uniform perturbation over layers  $p^l = p$  we focus on functions generated in the deep regime  $L \rightarrow \infty$ , where the order parameters take the form

$$m^l = \sum_{\{s_j\}} \prod_{j=1}^k \frac{1}{2} [1 + s_j m^{l-1} (1 - 2p)] \operatorname{sgn} \left[ \sum_{j=1}^k s_j \right], \quad (13)$$

$$q^l = \sum_{\{s_j, \hat{s}_j\}} \prod_{j=1}^k \frac{1}{4} [1 + \hat{s}_j m^{l-1} + s_j m^{l-1} (1 - 2p) + s_j \hat{s}_j q^{l-1} (1 - 2p)] \operatorname{sgn} \left[ \sum_{j=1}^k \hat{s}_j \right] \operatorname{sgn} \left[ \sum_{j=1}^k s_j \right]. \quad (14)$$

For finite  $k$ , the macroscopic observables at layer  $l$  are polynomially dependent on the observables at layer  $(l-1)$  up to order  $k$ . In the limit  $L \rightarrow \infty$ , the Boolean functions generated depend on the initial magnetization

$m^0 = \frac{1}{N} \sum_i s_i^0$ . Here, we consider a biased case with initial conditions  $\hat{m}^0 = m^0 > 0$  and  $q^0 = 1$ . The reference function admits a stationary solution  $\hat{m}^\infty = 1$ , computing a 1-bit information-preserving majority function [15]. Both magnetization of the perturbed function  $m^\infty$  and the function error  $\varepsilon = \frac{1}{2}(1 - q^\infty)$  exhibit a transition from the ordered phase to the paramagnetic phase at some critical perturbation level  $p_c$ , below which the perturbed network computes the reference function with error  $\varepsilon < \frac{1}{2}$ . The results for  $k=3$  are shown in Fig. 2(d). Interestingly, the critical perturbation  $p_c$  coincides with the location of the critical thermal noise  $\epsilon_c = \frac{1}{2}(1 - \tanh \beta_c)$  for noisy  $k$ -majority gate-based Boolean formulas; for  $k=3$ , the critical perturbation  $p_c = \frac{1}{6}$  [9]. Below  $p_c$ , there exist two ordered states with  $m^\infty = \pm \sqrt{(1-6p)/(1-2p)^3}$  and the overlap satisfies  $q^\infty = m^\infty$  [11], which is also reminiscent of the thermal noise-induced solutions [9]. However, the underlying physical implications are drastically different. Here it indicates that even in the deep network regime, there exists a large number  $\binom{Nk}{Nkp}^L$  of networks that can reliably represent the reference function when  $p < p_c$ . This function landscape is important for learning tasks to achieve a similar rule to the reference function. The propagation of internal error  $\delta(l) \equiv \frac{1}{2}(1 - q^l)$ , shown in Fig. 2(f), exhibits a stage of error-increase followed by a stage of error-decrease for  $p < p_c$ . Consequently *a successful DLM require more layers to reduce errors and provide a higher similarity to the reference function when we approach  $p_c$ , supporting current DLM practices.*

In summary, we propose a GF analysis to probe the function landscapes of DLM, focusing on the entropy of functions, given their error with respect to a reference function. The entropy maximization of densely connected networks at fixed error to the reference function indicates that weights of earlier layers are the first to align with reference function parameters when the error decreases. It highlights the importance of early-layer weights for reliable computation [16] and sheds light on the parameter learning-dynamics in function space during the learning process. We also investigate the phase transitions behavior in sparsely-connected networks, which advocate the use of deeper machines for suppressing errors with respect to the reference function. The suggested framework is very general and can easily accommodate different network structures and other computing elements. This is an important step towards a principled investigation of the typical behavior of DLM and we envisage follow up work on different aspects of the learning process.

We thank K. Y. Michael Wong for helpful discussions. Supports from The Leverhulme Trust (RPG-2013-48) (DS) and Research Grants Council of Hong Kong (Grants No. 605813 and No. 16322616) (BL) are acknowledged.



---

\* bliaf@connect.ust.hk

† d.saad@aston.ac.uk

- [1] M. Elad, “Deep, Deep Trouble,” *siam news*, <https://sinews.siam.org/Details-Page/deep-deep-trouble> (2017).
- [2] Y. LeCun, Y. Bengio, and G. Hinton, *Nature* **521**, 436 (2015).
- [3] E. Gardner, *Journal of Physics A: Mathematical and General* **21**, 257 (1988).
- [4] J. Hertz, A. Krogh, and R. Palmer, *Introduction To The Theory Of Neural Computation* (Addison-Wesley, 1991).
- [5] T. L. H. Watkin, A. Rau, and M. Biehl, *Rev. Mod. Phys.* **65**, 499 (1993).
- [6] D. Saad and S. A. Solla, *Phys. Rev. Lett.* **74**, 4337 (1995).
- [7] D. Saad, ed., *On-Line Learning in Neural Networks* (Cambridge University Press, 1998).
- [8] B. Poole, S. Lahiri, M. Raghu, J. Sohl-Dickstein, and S. Ganguli, in *Advances in Neural Information Processing Systems 29*, edited by D. D. Lee, M. Sugiyama, U. V. Luxburg, I. Guyon, and R. Garnett (Curran Associates, Inc., 2016) pp. 3360–3368.
- [9] A. Mozeika, D. Saad, and J. Raymond, *Phys. Rev. Lett.* **103**, 248701 (2009).
- [10] J. P. L. Hatchett, B. Wemmenhove, I. P. Castillo, T. Nikolettopoulos, N. S. Skantzos, and A. C. C. Coolen, *Journal of Physics A: Mathematical and General* **37**, 6201 (2004).
- [11] See supplementary material for details.
- [12] H. S. Seung, H. Sompolinsky, and N. Tishby, *Phys. Rev. A* **45**, 6056 (1992).
- [13] A. Engel and C. V. d. Broeck, *Statistical Mechanics of Learning* (Cambridge University Press, New York, 2001).
- [14] P. Savický, *Discrete Mathematics* **83**, 95 (1990).
- [15] A. Mozeika, D. Saad, and J. Raymond, *Phys. Rev. E* **82**, 041112 (2010).
- [16] M. Raghu, B. Poole, J. Kleinberg, S. Ganguli, and J. Sohl-Dickstein, in *Proceedings of the 34th International Conference on Machine Learning*, Proceedings of Machine Learning Research, Vol. 70, edited by D. Precup and Y. W. Teh (PMLR, International Convention Centre, Sydney, Australia, 2017) pp. 2847–2854.
-

# Exploring the Function Space of Deep-Learning Machines

## Supplementary Material

### A. Disorder Averaged Generating Functional for Densely-Connected Networks

Here we give detailed derivations of the generating functional for densely connected networks

$$\begin{aligned}
\Gamma[\hat{\boldsymbol{\psi}}, \boldsymbol{\psi}] &= \sum_{\{s_i^l, \hat{s}_i^l\}_{\forall l, i}} P(\hat{\boldsymbol{s}}^0) \prod_{i=1}^N \delta_{s_i^0, \hat{s}_i^0} \prod_{l=1}^L P(\hat{\boldsymbol{s}}^l | \hat{\boldsymbol{w}}^l, \hat{\boldsymbol{s}}^{l-1}) P(\boldsymbol{s}^l | \boldsymbol{w}^l, \boldsymbol{s}^{l-1}) e^{-i \sum_{l, i} (\hat{\psi}_i^l \hat{s}_i^l + \psi_i^l s_i^l)} \\
&= \sum_{\{s_i^l, \hat{s}_i^l\}_{\forall l, i}} P(\hat{\boldsymbol{s}}^0) \prod_i \delta_{s_i^0, \hat{s}_i^0} \prod_{l=1}^L \prod_i \frac{e^{\beta \hat{s}_i^l \hat{h}_i^l(\hat{\boldsymbol{w}}^l, \hat{\boldsymbol{s}}^{l-1})}}{2 \cosh [\beta \hat{h}_i^l(\hat{\boldsymbol{w}}^l, \hat{\boldsymbol{s}}^{l-1})]} \frac{e^{\beta s_i^l h_i^l(\boldsymbol{w}^l, \boldsymbol{s}^{l-1})}}{2 \cosh [\beta s_i^l h_i^l(\boldsymbol{w}^l, \boldsymbol{s}^{l-1})]} \\
&\quad \times e^{-i \sum_{l, i} (\hat{\psi}_i^l \hat{s}_i^l + \psi_i^l s_i^l)}, \tag{S1}
\end{aligned}$$

with the local field  $\hat{h}_i^l(\hat{\boldsymbol{w}}^l, \hat{\boldsymbol{s}}^{l-1}) = \frac{1}{\sqrt{N}} \sum_j \hat{w}_{ij}^l \hat{s}_j^{l-1}$ . To deal with the non-linearity of the local fields  $\hat{h}_i^l(\hat{\boldsymbol{w}}^l, \hat{\boldsymbol{s}}^{l-1})$  in the conditional probability, we introduce auxiliary fields through the integral representation of  $\delta$ -function

$$1 = \int_{-\infty}^{\infty} \frac{d\hat{h}_i^l d\hat{x}_i^l}{2\pi} e^{i\hat{x}_i^l (\hat{h}_i^l - \frac{1}{\sqrt{N}} \sum_j \hat{w}_{ij}^l \hat{s}_j^{l-1})}, \tag{S2}$$

$$1 = \int_{-\infty}^{\infty} \frac{dh_i^l dx_i^l}{2\pi} e^{ix_i^l (h_i^l - \frac{1}{\sqrt{N}} \sum_j w_{ij}^l s_j^{l-1})}, \tag{S3}$$

which allows us to express the quench random variables  $\hat{w}_{ij}^l$  and  $w_{ij}^l$  linearly in the exponents, leading to

$$\begin{aligned}
\Gamma[\hat{\boldsymbol{\psi}}, \boldsymbol{\psi}] &= \int \prod_{l=1}^L \prod_i \frac{d\hat{h}_i^l d\hat{x}_i^l}{2\pi} \frac{dh_i^l dx_i^l}{2\pi} \sum_{\{s_i^l, \hat{s}_i^l\}_{\forall l, i}} P(\hat{\boldsymbol{s}}^0) \prod_i \delta_{s_i^0, \hat{s}_i^0} e^{-i \sum_{l, i} (\hat{\psi}_i^l \hat{s}_i^l + \psi_i^l s_i^l)} \\
&\quad \times \exp \left\{ \frac{-i}{\sqrt{N}} \sum_{l=1}^L \left[ \sum_{ij} \hat{w}_{ij}^l \hat{x}_i^l \hat{s}_j^{l-1} + \sum_{ij} w_{ij}^l x_i^l s_j^{l-1} \right] \right\} \tag{S4}
\end{aligned}$$

$$\begin{aligned}
&\quad \times \exp \left\{ \sum_{l=1}^L \sum_i \left[ \beta \hat{s}_i^l \hat{h}_i^l + \beta s_i^l h_i^l - \log 2 \cosh \beta \hat{h}_i^l - \log 2 \cosh \beta h_i^l + i\hat{x}_i^l \hat{h}_i^l + ix_i^l h_i^l \right] \right\}. \tag{S5}
\end{aligned}$$

Assuming the system is self-averaging, the disorder average can be traced over *ab initio* [S1], leaving the disorder averaged generating functional  $\Gamma[\hat{\boldsymbol{\psi}}, \boldsymbol{\psi}]$ . We consider two types of networks, one with continuous weight variable following a Gaussian distribution and the other with binary weight variables. In both cases, we consider input distribution of the form

$$P(\hat{\boldsymbol{s}}^0) = \prod_i P(\hat{s}_i^0) = \prod_i \left( \frac{1}{2} \delta_{\hat{s}_i^0, 1} + \frac{1}{2} \delta_{\hat{s}_i^0, -1} \right). \tag{S6}$$

#### 1. Continuous weight variables with Gaussian disorder

In this case, we assume that weight variables are independent and follow a Gaussian density  $\hat{w}_{ij}^l \sim \mathcal{N}(0, \sigma^2)$ , and that the perturbed weight has the form  $w_{ij}^l = \sqrt{1 - (\eta^l)^2} \hat{w}_{ij}^l + \eta^l \delta w_{ij}^l$  where  $\delta w_{ij}^l$  also have density  $\mathcal{N}(0, \sigma^2)$  but is

independent of  $\hat{w}_{ij}^l$ . Averaging Eq. (S4) over the weight  $\{\hat{w}_{ij}^l\}$  and perturbation  $\{\delta w_{ij}^l\}$  gives

$$\begin{aligned} & \int P(\hat{\mathbf{w}})P(\delta\mathbf{w})d\hat{\mathbf{w}} d\delta\mathbf{w} \exp \left\{ \frac{-i}{\sqrt{N}} \sum_{l=1}^L \left[ \sum_{ij} \hat{w}_{ij}^l \left( \hat{x}_i^l \hat{s}_j^{l-1} + \sqrt{1 - (\eta^l)^2} x_i^l \hat{s}_j^{l-1} \right) + \eta^l \sum_{ij} \delta w_{ij}^l x_i^l \hat{s}_j^{l-1} \right] \right\} \\ & = \exp \left\{ -\sigma^2 \sum_{l=1}^L \left[ \frac{1}{2} \sum_i (\hat{x}_i^l)^2 + \frac{1}{2} \sum_i (x_i^l)^2 + \sqrt{1 - (\eta^l)^2} \sum_i \hat{x}_i^l x_i^l \left( \sum_j \frac{1}{N} \hat{s}_j^{l-1} s_j^{l-1} \right) \right] \right\}, \end{aligned} \quad (\text{S7})$$

leading to the disorder-averaged generating functional

$$\begin{aligned} \overline{\Gamma[\hat{\boldsymbol{\psi}}, \boldsymbol{\psi}]} &= \int \prod_{l=1}^L \prod_i \frac{d\hat{h}_i^l d\hat{x}_i^l}{2\pi} \frac{dh_i^l dx_i^l}{2\pi} \sum_{\{\hat{s}_i^l, s_i^l\}_{\forall l, i}} P(\hat{\mathbf{s}}^0) \prod_i \delta_{\hat{s}_i^0, s_i^0} e^{-i \sum_{l,i} (\hat{\psi}_i^l \hat{s}_i^l + \psi_i^l s_i^l)} \\ & \times \exp \left\{ -\sigma^2 \sum_{l=1}^L \left[ \frac{1}{2} \sum_i (\hat{x}_i^l)^2 + \frac{1}{2} \sum_i (x_i^l)^2 + \sqrt{1 - (\eta^l)^2} \sum_i \hat{x}_i^l x_i^l \left( \sum_j \frac{1}{N} \hat{s}_j^{l-1} s_j^{l-1} \right) \right] \right\} \\ & \times \exp \left\{ \sum_{l=1}^L \sum_i \left[ \beta \hat{s}_i^l \hat{h}_i^l + \beta s_i^l h_i^l - \log 2 \cosh \beta \hat{h}_i^l - \log 2 \cosh \beta h_i^l + i \hat{x}_i^l \hat{h}_i^l + i x_i^l h_i^l \right] \right\}. \end{aligned} \quad (\text{S8})$$

Site factorization can be achieved by defining the macroscopic order parameter  $q^l := \sum_j \frac{1}{N} \hat{s}_j^l s_j^l$  through the integral representation of the  $\delta$ -function

$$1 = \int \frac{d\mathcal{Q}^l dq^l}{2\pi/N} \exp \left\{ iN \mathcal{Q}^l \left[ q^l - \frac{1}{N} \sum_i s_i^l \hat{s}_i^l \right] \right\}, \quad (\text{S9})$$

which leads to

$$\begin{aligned} \overline{\Gamma[\hat{\boldsymbol{\psi}}, \boldsymbol{\psi}]} &= \int \prod_{l=0}^L \frac{d\mathcal{Q}^l dq^l}{2\pi/N} \exp \left\{ iN \sum_{l=0}^L \mathcal{Q}^l q^l \right\} \\ & \times \int \prod_{l=1}^L \prod_i \frac{d\hat{h}_i^l d\hat{x}_i^l}{2\pi} \frac{dh_i^l dx_i^l}{2\pi} \sum_{\{\hat{s}_i^l, s_i^l\}_{\forall l, i}} P(\hat{\mathbf{s}}^0) \prod_i \delta_{\hat{s}_i^0, s_i^0} e^{-i \sum_{l,i} (\hat{\psi}_i^l \hat{s}_i^l + \psi_i^l s_i^l)} \\ & \times \exp \left\{ -\sigma^2 \sum_{l=1}^L \left[ \frac{1}{2} \sum_i (\hat{x}_i^l)^2 + \frac{1}{2} \sum_i (x_i^l)^2 + \sqrt{1 - (\eta^l)^2} \sum_i \hat{x}_i^l x_i^l q^{l-1} \right] \right\} \\ & \times \exp \left\{ \sum_{l=1}^L \sum_i \left[ \beta \hat{s}_i^l \hat{h}_i^l + \beta s_i^l h_i^l - \log 2 \cosh \beta \hat{h}_i^l - \log 2 \cosh \beta h_i^l + i \hat{x}_i^l \hat{h}_i^l + i x_i^l h_i^l \right] \right\} \\ & \times \exp \left( -i \sum_{l=0}^L \sum_i \mathcal{Q}^l \hat{s}_i^l s_i^l \right). \end{aligned} \quad (\text{S10})$$

Now the spin and field variables are the same for any site  $i$  and integrate over the auxiliary variable, resulting in

$$\begin{aligned}
\overline{\Gamma[\hat{\psi}, \psi]} &= \int \prod_{l=0}^L \frac{d\mathcal{Q}^l dq^l}{2\pi/N} \exp \left\{ iN \sum_{l=0}^L \mathcal{Q}^l q^l \right\} \\
&\times \left\{ \int \prod_{l=1}^L \frac{d\hat{h}^l d\hat{x}^l}{2\pi} \frac{dh^l dx^l}{2\pi} \sum_{\{\hat{s}^l, s^l\}_{\forall l}} P(\hat{\mathbf{s}}^0) \delta_{\hat{s}^0, s^0} e^{-i \sum_l (\hat{\psi}^l \hat{s}^l + \psi^l s^l)} \right. \\
&\times \exp \left( -\sigma^2 \sum_{l=1}^L \left[ \frac{1}{2} (\hat{x}^l)^2 + \frac{1}{2} (x^l)^2 + \sqrt{1 - (\eta^l)^2} \hat{x}^l x^l q^{l-1} \right] + i \sum_{l=1}^L (\hat{x}^l \hat{h}^l + x^l h^l) \right) \\
&\times \exp \left( \sum_{l=1}^L \left[ \beta \hat{s}^l \hat{h}^l + \beta s^l h^l - \log 2 \cosh \beta \hat{h}^l - \log 2 \cosh \beta h^l \right] \right) \\
&\times \exp \left( -i \sum_{l=0}^L \mathcal{Q}^l \hat{s}^l s^l \right) \left. \right\}^N. \tag{S11}
\end{aligned}$$

$$\begin{aligned}
&\times \exp \left( -i \sum_{l=0}^L \mathcal{Q}^l \hat{s}^l s^l \right) \left. \right\}^N. \tag{S12}
\end{aligned}$$

For convenience, we define the fields doublet  $X^l := [\hat{x}^l, x^l]^T$ ,  $H^l := [\hat{h}^l, h^l]^T$  and the correlation matrix

$$\Sigma_l(\eta^l, q^{l-1}) = \sigma^2 \begin{bmatrix} 1 & \sqrt{1 - (\eta^l)^2} q^{l-1} \\ \sqrt{1 - (\eta^l)^2} q^{l-1} & 1 \end{bmatrix}. \tag{S13}$$

The density of  $\{\hat{x}^l, x^l\}$  in Eq. (S11) has the form  $\exp\{-\sum_l [\frac{1}{2}(X^l)^T \cdot \Sigma_l \cdot X^l + i(X^l)^T \cdot H^l]\}$ , which can be integrated over  $\{X^l\}$ , yielding the joint Gaussian density of  $H^l$  with precision matrix  $\Sigma_l^{-1}$

$$\frac{1}{\sqrt{(2\pi)^2 |\Sigma_l|}} \exp \left\{ -\sum_l \frac{1}{2} (H^l)^T \cdot \Sigma_l(\eta^l, q^{l-1})^{-1} \cdot H^l \right\}. \tag{S14}$$

## 2. Binary weight variables

For the binary weight variables, we assume a disorder of the form  $P(\hat{w}_{ij}^l) = \frac{1}{2} \delta_{\hat{w}_{ij}^l, 1} + \frac{1}{2} \delta_{\hat{w}_{ij}^l, -1}$ ,  $P(w_{ij}^l) = (1 - p^l) \delta_{w_{ij}^l, \hat{w}_{ij}^l} + p^l \delta_{w_{ij}^l, -\hat{w}_{ij}^l}$ , where  $p^l$  is the flipping probability at layer  $l$ . Averaging Eq. (S4) over the weight  $\{\hat{w}_{ij}^l\}$  and the perturbation  $\{\delta w_{ij}^l\}$  gives

$$\begin{aligned}
&\prod_{l=1}^L \prod_{ij} \left[ (1 - p^l) \cos \left( \frac{1}{\sqrt{N}} (\hat{x}_i^l \hat{s}_j^{l-1} + x_i^l s_j^{l-1}) \right) + p^l \cos \left( \frac{1}{\sqrt{N}} (\hat{x}_i^l \hat{s}_j^{l-1} - x_i^l s_j^{l-1}) \right) \right] \\
&\approx \prod_{l=1}^L \prod_{ij} \left[ (1 - p^l) \left[ 1 - \frac{1}{2N} (\hat{x}_i^l \hat{s}_j^{l-1} + x_i^l s_j^{l-1})^2 \right] + p^l \left[ 1 - \frac{1}{2N} (\hat{x}_i^l \hat{s}_j^{l-1} - x_i^l s_j^{l-1})^2 \right] \right] \\
&\approx \prod_{l=1}^L \prod_{ij} \exp \left\{ -\frac{1}{2N} [(\hat{x}_i^l)^2 + (x_i^l)^2 + 2(1 - 2p^l) \hat{x}_i^l x_i^l \hat{s}_j^{l-1} s_j^{l-1}] \right\} \\
&= \exp \left\{ -\sum_{l=1}^L \sum_i \left[ \frac{1}{2} (\hat{x}_i^l)^2 + \frac{1}{2} (x_i^l)^2 + (1 - 2p^l) \hat{x}_i^l x_i^l \left( \sum_j \frac{1}{N} \hat{s}_j^{l-1} s_j^{l-1} \right) \right] \right\}, \tag{S15}
\end{aligned}$$

where the large  $N$  property is used in the second and third line. The resulting density is similar to the density of the continuous weight variables in Eq. (S7), and therefore the same derivations can be applied. By identifying the correlation matrix

$$\Sigma_l(p^l, q^{l-1}) = \begin{bmatrix} 1 & (1 - 2p^l) q^{l-1} \\ (1 - 2p^l) q^{l-1} & 1 \end{bmatrix}, \tag{S16}$$

the density for the site independent local field  $H^l$  also has the Gaussian density in the form of

$$\frac{1}{\sqrt{(2\pi)^2 |\Sigma_l|}} \exp \left\{ -\sum_l \frac{1}{2} (H^l)^T \cdot \Sigma_l(p^l, q^{l-1})^{-1} \cdot H^l \right\}. \tag{S17}$$



### 3. Effective single site measure and saddle point equations

In summary, the cases of continuous weight variables and binary weight variables have the unified expressions by properly identifying the correlation matrix for the local fields  $\{H^l\}$ . The generating functional in both cases has the form

$$\bar{\Gamma} = \int \prod_{l=0}^L \frac{d\mathcal{Q}^l dq^l}{2\pi/N} e^{N\Psi[\mathbf{q}, \mathcal{Q}]}, \quad (\text{S18})$$

with the exponent

$$\Psi[\mathbf{q}, \mathcal{Q}] = i \sum_{l=0}^L \mathcal{Q}^l q^l + \log \int \prod_{l=1}^L d\hat{h}^l dh^l \sum_{\{\hat{s}^l, s^l\}} M[\hat{s}, s, \hat{h}, h], \quad (\text{S19})$$

and the effective single site measure  $M[\dots]$  has the form of

$$M[\{\hat{s}^l, s^l, \hat{h}^l, h^l\}] = P(\hat{s}^0) \delta_{\hat{s}^0, s^0} e^{-i \sum_{l=0}^L \mathcal{Q}^l \hat{s}^l s^l} e^{-i \sum_l (\hat{\psi}^l \hat{s}^l + \psi^l s^l)} \\ \times \prod_{l=1}^L \left\{ \frac{e^{\beta \hat{s}^l \hat{h}^l}}{2 \cosh \beta \hat{h}^l} \frac{e^{\beta s^l h^l}}{2 \cosh \beta h^l} \frac{1}{\sqrt{(2\pi)^2 |\Sigma_l(q^{l-1})|}} \exp \left[ -\frac{1}{2} (H^l)^T \cdot \Sigma_l(q^{l-1})^{-1} \cdot H^l \right] \right\} \quad (\text{S20})$$

Now that the potential  $\Psi[\dots]$  is expressed by macroscopic order parameters  $\{\mathcal{Q}^l, q^l\}$ , the conjugate fields  $\{\hat{\psi}^l, \psi^l\}$  in Eq. (S20) can be omitted. For  $N \rightarrow \infty$ ,  $\bar{\Gamma}$  is dominated by the extremum of  $\Psi[\mathbf{q}, \mathcal{Q}]$  given by  $\partial\Psi/\partial\mathcal{Q}^l = 0$  and  $\partial\Psi/\partial q^l = 0$

$$q^l = \langle \hat{s}^l s^l \rangle_{M[\dots]} \\ = \frac{\int \prod_{l=1}^L d\hat{h}^l dh^l \sum_{\{\hat{s}^l, s^l\}} \hat{s}^l s^l M[\{\hat{s}^l, s^l, \hat{h}^l, h^l\}]}{\int \prod_{l=1}^L d\hat{h}^l dh^l \sum_{\{\hat{s}^l, s^l\}} M[\{\hat{s}^l, s^l, \hat{h}^l, h^l\}]} \quad (\text{S21})$$

$$i\mathcal{Q}^l = -\frac{\int \prod_{l=1}^L d\hat{h}^l dh^l \sum_{\{\hat{s}^l, s^l\}} \frac{\partial}{\partial q^l} M[\{\hat{s}^l, s^l, \hat{h}^l, h^l\}]}{\int \prod_{l=1}^L d\hat{h}^l dh^l \sum_{\{\hat{s}^l, s^l\}} M[\{\hat{s}^l, s^l, \hat{h}^l, h^l\}]} \quad (\text{S22})$$

Since the two systems are interlinked through the input vectors  $\delta_{\hat{s}^0, s^0}$  and the final overlap  $q^L$  does not show up in the measure  $M[\dots]$ , the saddle point equations Eq. (S21) and Eq. (S22) have the boundary conditions

$$q^0 = 1, \quad (\text{S23})$$

$$i\mathcal{Q}^L = 0. \quad (\text{S24})$$

### 4. Simplifications of the saddle point equations

The saddle point of  $i\mathcal{Q}^l$  can be further simplified by iterating backward from the boundary condition Eq. (S24). We start from computing  $i\mathcal{Q}^{L-1}$  by substituting Eq. (S24) into Eq. (S22)

$$i\mathcal{Q}^{L-1} = -\frac{\int d\hat{h}^L dh^L \frac{\partial}{\partial q^{L-1}} \left\{ \frac{1}{\sqrt{(2\pi)^2 |\Sigma_L(q^{L-1})|}} \exp \left[ -\frac{1}{2} (H^L)^T \cdot \Sigma_L(q^{L-1})^{-1} \cdot H^L \right] \right\}}{\int d\hat{h}^L dh^L \frac{1}{\sqrt{(2\pi)^2 |\Sigma_L(q^{L-1})|}} \exp \left[ -\frac{1}{2} (H^L)^T \cdot \Sigma_L(q^{L-1})^{-1} \cdot H^L \right]} \\ = -\int dH^L \frac{\partial}{\partial q^{L-1}} \left\{ \int \frac{dX}{(2\pi)^2} \exp \left[ -\frac{1}{2} X^T \cdot \Sigma_L(q^{L-1}) \cdot X + iX \cdot H^L \right] \right\} \\ = \frac{1}{(2\pi)^2} \frac{\partial \Sigma_{L,12}(q^{L-1})}{\partial q^{L-1}} \int dH^L dX(\hat{x}x) \exp \left[ -\frac{1}{2} X^T \cdot \Sigma_L(q^{L-1}) \cdot X + iX \cdot H^L \right], \quad (\text{S25})$$

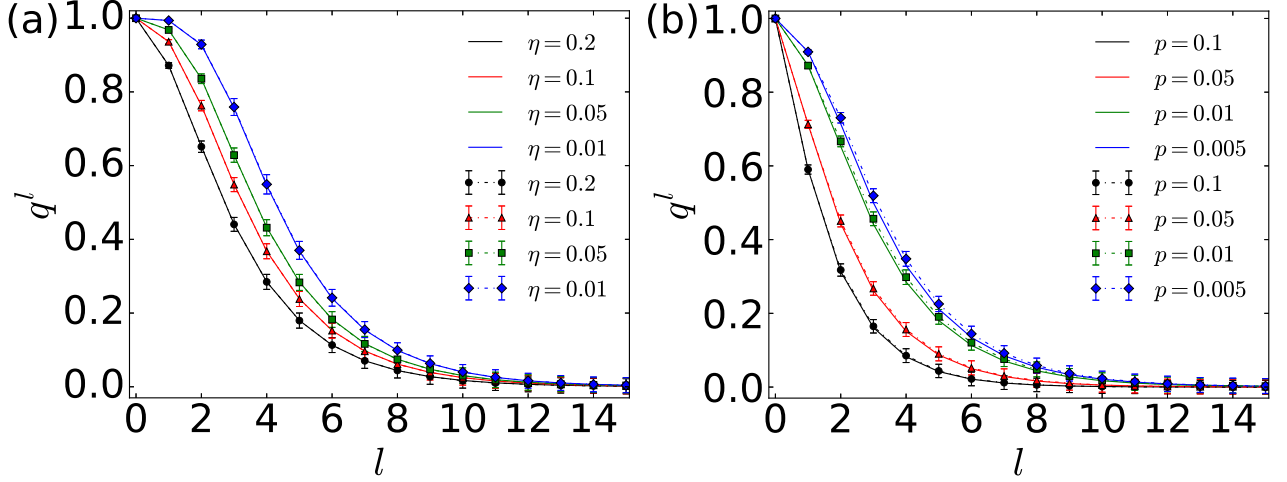


Figure S1. Comparison of the overlap evolution in layers of Eq. (S29) (solid lines) to Monte Carlo simulations (dashed-dotted lines with markers), which shows a perfect match between the two approaches. The perturbations are homogeneous in both cases, i.e.,  $\eta^l = \eta$  and  $p^l = p$ . The systems are of size  $N = 4000$  and the results are averaged over 100 disorder realizations. (a) Continuous weight variables. (b) Binary weight variables.

where  $\partial \Sigma_{L,12}(q^{L-1})/\partial q^{L-1} = \sigma^2 \sqrt{1 - (\eta^L)^2}$  for continuous weights and  $\partial \Sigma_{L,12}(q^{L-1})/\partial q^{L-1} = 1 - 2p^l$  for binary weights. Further notice that

$$\begin{aligned}
 & \int dH^L dX(\hat{x}x) \exp \left[ -\frac{1}{2} X^T \cdot \Sigma_L(q^{L-1}) \cdot X + iX \cdot H^L \right] \\
 &= (2\pi)^2 \int dX(\hat{x}x) \delta(\hat{x}) \delta(x) \exp \left[ -\frac{1}{2} X^T \cdot \Sigma_L(q^{L-1}) \cdot X \right] \\
 &= 0,
 \end{aligned} \tag{S26}$$

giving  $iQ^{L-1} = 0$ . This can be used to show that  $iQ^{L-2} = 0$  etc and finally we conclude that in the saddle point

$$iQ^l = 0, \quad \forall l. \tag{S27}$$

Therefore the overlap  $q^l$  can be simplified as

$$q^l = \int d\hat{h}^l dh^l \tanh(\beta \hat{h}^l) \tanh(\beta h^l) \frac{1}{\sqrt{(2\pi)^2 |\Sigma_l(q^{l-1})|}} \exp \left[ -\frac{1}{2} (H^l)^T \cdot \Sigma_l(q^{l-1})^{-1} \cdot H^l \right]. \tag{S28}$$

Consider the deterministic limit  $\beta \rightarrow \infty$ ,  $\tanh(\beta h^l) \rightarrow \text{sgn}(h^l)$ , the double integration in Eq. (S28) can be carried out analytically, yielding

$$\begin{aligned}
 q^l &= \frac{2}{\pi} \tan^{-1} \left( \frac{\Sigma_{l,12}(q^{l-1})}{\sqrt{|\Sigma_l(q^{l-1})|}} \right) \\
 &= \begin{cases} \frac{2}{\pi} \sin^{-1} \left( \sqrt{1 - (\eta^l)^2} q^{l-1} \right), & \text{continuous weights,} \\ \frac{2}{\pi} \sin^{-1} \left( (1 - 2p^l) q^{l-1} \right), & \text{binary weights.} \end{cases}
 \end{aligned} \tag{S29}$$

The mean field overlap evolution in layers of Eq. (S29) are perfectly confirmed by Monte Carlo simulations as shown in Fig. S1.

## B. Maximum-Entropy Perturbation

In this section we describe the procedure for finding the dominating entropy spread for a given generalization error in the continuous-weight scenario

$$\max_{\{\eta^l\}} S_{\text{con}}(\{\eta^l\}) = \frac{1}{L} \sum_{l=1}^L \log \eta^l, \quad (\text{S30})$$

$$\text{s.t. } q^L(\{\eta^l\}) = 1 - 2\varepsilon. \quad (\text{S31})$$

To ease the nonlinear function-composition constraint in Eq. (S31), we first notice in Eq. (S29) that  $q^l$  is a monotonic function of  $\eta^l$  which allows us to express  $\eta^l$  as

$$\eta^l(q^{l-1}, q^l) = \sqrt{1 - \frac{\sin^2(\frac{\pi}{2}q^l)}{(q^{l-1})^2}}, \quad (\text{S32})$$

with  $\sin(\frac{\pi}{2}q^l) \leq q^{l-1}$ . Then the maximization problem can be recast as

$$\max_{\{q^l\}} S_{\text{con}}(\{\eta^l(q^{l-1}, q^l)\}) = \frac{1}{L} \sum_{l=1}^L \log \eta^l(q^{l-1}, q^l), \quad (\text{S33})$$

$$\begin{aligned} \text{s.t. } \quad & \sin(\frac{\pi}{2}q^l) \leq q^{l-1}, \quad l = 1, \dots, L \\ & q^0 = 1, \\ & q^L = 1 - 2\varepsilon, \end{aligned} \quad (\text{S34})$$

which can be solved numerically. The inequality constraints in Eq. (S34) are non-convex and the minimizers  $\{q^{*l}\}$  found are possibly local minima. We start from multiple initial guesses and select the best solution obtained. Then the maximum-entropy perturbations are given by  $\eta^{*l} = \eta^l(q^{*l-1}, q^{*l})$ . We denote the corresponding optimal entropy at distance- $\varepsilon$  from the reference function as  $S_{\text{con}}^*(\varepsilon)$ .

The procedures for the binary-weight problem are similar, with the perturbation expressed in overlaps as

$$p^l(q^{l-1}, q^l) = \frac{1}{2} \left( 1 - \frac{\sin(\frac{\pi}{2}q^l)}{q^{l-1}} \right). \quad (\text{S35})$$

The abrupt transition of the maximum-entropy perturbations  $\{p^{*l}\}$  comes from the transitions of the global maximum of  $S_{\text{bin}}(\{p^l(q^{l-1}, q^l)\})$  from the interior of the feasible region to its boundary. An example of such jump in the maximum for a system with  $L = 3$  is illustrated in Fig S2. This jump in entropy maximum is reminiscent of the shift of free energy minimum occurred in first order phase transitions.

### C. The Annealed Approximation of Learning

In this section we give more details of the annealed approximation of learning [S2, S3]. The  $(L + 1)$ -layer network constructed here maps an  $N$ -dimensional input  $\{s_i^0\}_{i=1, \dots, N}$  to an  $N$ -dimensional output  $\{s_i^L\}_{i=1, \dots, N}$ , where each component  $s_i^L$  is the output of a certain Boolean function with  $N$  dimensional input, e.g., a single instance of a binary classifier. Therefore all the  $N$  components of the  $\mathbf{s}^L$  are the outputs of  $N$  weakly coupled Boolean functions that share the same typical properties.

Consider the case of densely-connected networks with continuous weights. We start by showing how the profile of the typical phase volume  $\Omega_{\text{tot}}(\{\eta^{*l}\}, \varepsilon)$  is re-shaped by the constraints represented by the introduction of examples. The function distance (error)  $\varepsilon$  we defined is closely related to the generalization error in supervised learning. Suppose a randomly chosen example (input-output pair provided by the reference function) is introduced, the distance- $\varepsilon$  functions on average has probability  $\varepsilon$  of providing the wrong output based on the input of the introduced example. On average,  $(1 - \varepsilon)$ -fraction of the  $\Omega_{\text{tot}}(\{\eta^{*l}\}, \varepsilon)$  solutions are compatible with the present example; therefore the remaining volume of compatible solutions is  $\Omega_{\text{tot}}(\{\eta^{*l}\}, \varepsilon)(1 - \varepsilon)$ . High- $\varepsilon$  functions are ruled out faster, resulting in increasing concentration of the low- $\varepsilon$  functions. This learning process is illustrated in Fig. S3(a).

Assuming the examples are weakly correlated, the phase volume at the presence of  $P = \alpha LN^2$  examples using the annealed approximation is given by  $\Omega_\alpha(\varepsilon) = \Omega_{\text{tot}}(\{\eta^{*l}\}, \varepsilon)(1 - \varepsilon)^P$ . The corresponding annealed entropy density is

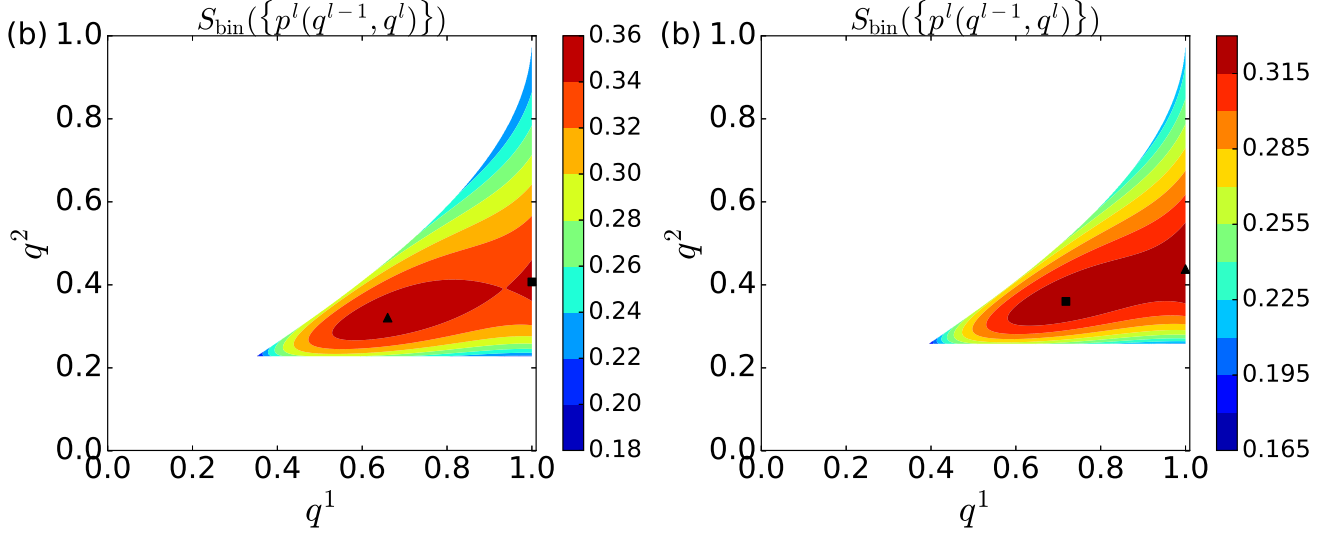


Figure S2. Entropy of  $L = 3$  binary-weight networks  $S_{\text{bin}}(\{p^l(q^{l-1}, q^l)\})$  as a function of the internal-layer overlap  $q^1$  and  $q^2$ . The input and output overlaps are fixed as  $q^0 = 1$  and  $q^{L=3} = 1 - 2\varepsilon$ . The global maximum is marked as a triangle and the local but not global maximum is marked as a square. (a)  $\varepsilon = 0.427$ ; there exist two local maxima and the global maximum is located in the interior of the feasible region. (b)  $\varepsilon = 0.417$ ; the global maximum jumps from the interior to the boundary of the feasible region with  $q^1 = 1$ ; it indicates  $p^{*1} = 0$ , i.e., the first-layer weights match with that of the reference network perfectly  $\mathbf{w}^1 = \hat{\mathbf{w}}^1$ .

$S_\alpha(\varepsilon) = \log \Omega_\alpha(\varepsilon)/(LN^2) = S_{\text{con}}^*(\varepsilon) + \alpha \log(1 - \varepsilon)$ . In the large  $N$  limit, the generalization error can be obtained by

$$\begin{aligned} \varepsilon^*(\alpha) &= \operatorname{argmax}_\varepsilon \Omega_\alpha(\varepsilon) \\ &= \operatorname{argmax}_\varepsilon S_\alpha(\varepsilon). \end{aligned} \quad (\text{S36})$$

The learning process in a network of  $L = 2$  is illustrated in Fig. S3(b).

Although the generalization curve obtained by the annealed learning theory is only an approximation, it produces the correct qualitative behaviors in many cases, e.g., the large  $\alpha$  scaling [S3]. We also note that our derivation is based on the small perturbation limit. Therefore, we expect the obtained generalization curves are more relevant in the small  $\varepsilon$  (large  $\alpha$ ) limit.

#### D. Saddle Point Equations for Sparsely-Connected Networks

The calculations of the sparsely connected binary networks are similar to the densely-connected case, except that the local fields are only contributed by finite number of elements  $\hat{h}_i^l(A^l, \hat{\mathbf{w}}^l, \hat{\mathbf{s}}^{l-1}) = \frac{1}{\sqrt{k}} \sum_j A_{ij}^l \hat{w}_{ij}^l \hat{s}_j^{l-1}$  where  $A_{ij}^l$  is the connectivity matrix between layer  $l-1$  and layer  $l$  satisfying  $\sum_j A_{ij}^l = k$ ; this induces additional disorder of a different type. Such network topology is used in previous studies of random Boolean formula [S4]. To make use of the steps of calculations therein, we adapt the notion of adjacency matrix  $A_{ij}^l$  to the connectivity tensor as  $A_{i_1, \dots, i_k}^{l,i}$ , indicating the  $i$ -th neuron at layer  $l$  is connected to the neurons at  $(l-1)$ -th layer with indices  $i_1, \dots, i_k$ . The local field is expressed as

$$\begin{aligned} \hat{h}_i^l(A^{l,i}, \hat{\mathbf{w}}^l, \hat{\mathbf{s}}^{l-1}) &= \frac{1}{\sqrt{k}} \left( A_{j_1, j_2, \dots, j_k}^{l,i} \hat{w}_{i j_1}^l \hat{s}_{j_1}^{l-1} + A_{j_1, j_2, \dots, j_k}^{l,i} \hat{w}_{i j_2}^l \hat{s}_{j_2}^{l-1} + \dots + A_{j_1, j_2, \dots, j_k}^{l,i} \hat{w}_{i j_k}^l \hat{s}_{j_k}^{l-1} \right), \\ &:= A_{j_1, j_2, \dots, j_k}^{l,i} \hat{\alpha}_{\hat{\mathbf{w}}^l}^{l,i}(\hat{s}_{j_1}^{l-1}, \hat{s}_{j_2}^{l-1}, \dots, \hat{s}_{j_k}^{l-1}), \end{aligned} \quad (\text{S37})$$

where we have introduced the notation  $\hat{\alpha}_{\hat{\mathbf{w}}^l}^{l,i}$  to mimic the gate output of Boolean formula as in Ref. [S4].

The connectivity tensor follows the probability distribution

$$P(\{A_{i_1, \dots, i_k}^{l,i}\}) = \frac{1}{Z_A} \prod_{l=1}^L \prod_i \left\{ \delta \left( \sum_{j_1, \dots, j_k} A_{j_1, \dots, j_k}^{l,i}, 1 \right) \prod_{i_1, \dots, i_k} \left[ \frac{1}{N^k} \delta_{A_{i_1, \dots, i_k}^{l,i}, 1} + \left(1 - \frac{1}{N^k}\right) \delta_{A_{i_1, \dots, i_k}^{l,i}, 0} \right] \right\}, \quad (\text{S38})$$

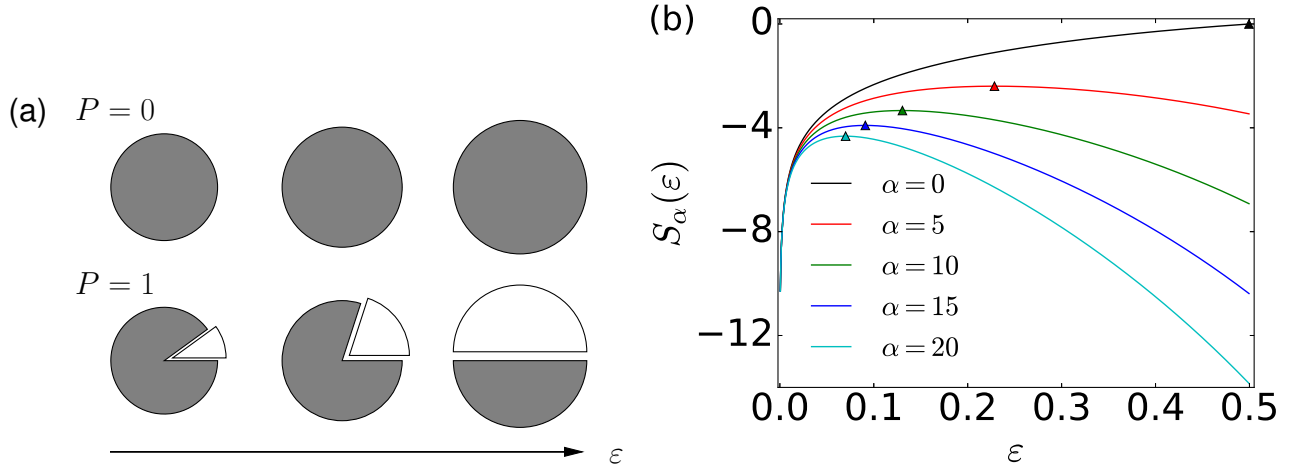


Figure S3. (a) Schematic illustration of the annealed learning process. The dark area represents the phase volume compatible with the examples at a given level of generalization error  $\varepsilon$ . Upper row corresponds to the case where no example is present. In the lower row, a single example is introduced and the phase volume is re-shaped as  $\Omega_1(\varepsilon) = \Omega_0(\varepsilon)(1 - \varepsilon)$ ; on average more high- $\varepsilon$  functions are incompatible with the example than the low- $\varepsilon$  functions, which will be ruled out in the learning process (marked as white regions removed). It results in the increased concentration of low- $\varepsilon$  functions. (b) The annealed entropy density  $S_\alpha(\varepsilon)$  vs  $\varepsilon$  for different  $\alpha$  values. The two layer network ( $L = 2$ ) is densely-connected with continuous-weight variables. The space of candidate functions is dominated by functions that maximize the entropy  $S_\alpha(\varepsilon)$  for a particular  $\alpha$  value, marked by a triangle.

where  $Z_A$  is the normalization factor. In Eq. (S38) we have made use of the fact that the probability of having the same indices in  $\{i_1, i_2, \dots, i_k\}$  of  $A_{i_1, \dots, i_k}^{l, i}$  vanishes in the limit  $N \rightarrow \infty$ , or the fact that  $\frac{1}{N(N-1)\dots(N-k+1)} \approx \frac{1}{N^k}$  for finite  $k$ .

The average over the connectivity follows exactly the same procedures as in Ref. [S4] and the average over weight disorder  $P(\hat{w})$  and  $P(w)$  can be viewed as an average over the gate disorder  $\hat{\alpha}_{\hat{w}}$  and  $\alpha_w$ . With the help of the functional order parameter  $\mathcal{P}^l(\hat{s}, s) := \frac{1}{N} \sum_i \delta_{\hat{s}_i^l, \hat{s}} \delta_{s_i^l, s}$  relating the magnetization  $m^l := \frac{1}{N} \sum_i s_i^l$  and overlap  $q^l$  through

$$\mathcal{P}^l(\hat{s}, s) = \frac{1}{4}(1 + \hat{s}\hat{m}^l + sm^l + \hat{s}s q^l), \quad (\text{S39})$$

we are eventually led to the self-consistent saddle point equation [S4]

$$\mathcal{P}^l(\hat{s}, s) = \langle \delta_{\hat{s}^l, \hat{s}} \delta_{s^l, s} \rangle_{M[\dots]}, \quad (\text{S40})$$

with the effective single-site measure

$$M[\{\hat{s}^l, s^l\}] = P(\hat{s}^0) \delta_{\hat{s}^0, s^0} \prod_{l=1}^L \left\{ \sum_{\{\hat{s}_j, s_j\}} \prod_{j=1}^k \mathcal{P}^l(\hat{s}_j, s_j) \times \left\langle \frac{\exp[\beta \hat{s}^l \hat{\alpha}_{\hat{w}}(\hat{s}_1, \hat{s}_2, \dots, \hat{s}_k)] \exp[\beta s^l \alpha_w(s_1, s_2, \dots, s_k)]}{2 \cosh[\beta \hat{\alpha}_{\hat{w}}(\hat{s}_1, \hat{s}_2, \dots, \hat{s}_k)] 2 \cosh[\beta s^l \alpha_w(s_1, s_2, \dots, s_k)]} \right\rangle_{\hat{\alpha}_{\hat{w}}, \alpha_w} \right\}. \quad (\text{S41})$$

Note the spin variables  $s_j$ ,  $s^l$  and  $s$  in this section are different objects. From a physical point of view, the dynamical variable  $s^l$  at layer  $l$  experiences a local field  $\alpha_w(s_1, s_2, \dots, s_k)$  contributed by “dummy spins”  $\{s_1, s_2, \dots, s_k\}$  which reflects the mean field interactions from  $k$  spins from layer  $l - 1$ . The macroscopic variables  $s, \hat{s}$  are defined to express the magnetizations and overlaps.

By using Eqs. (S39), (S40) and (S41), the evolution of magnetization and overlap reads

$$\hat{m}^l = \sum_{\{\hat{s}_j\}} \prod_{j=1}^k \left[ \frac{1 + \hat{s}_j \hat{m}^{l-1}}{2} \right] \langle \tanh[\beta \hat{\alpha}_{\hat{w}}(\hat{s}_1, \hat{s}_2, \dots, \hat{s}_k)] \rangle_{\hat{\alpha}_{\hat{w}}}, \quad (\text{S42})$$

$$m^l = \sum_{\{s_j\}} \prod_{j=1}^k \left[ \frac{1 + s_j m^{l-1}}{2} \right] \langle \tanh [\beta \alpha_w (s_1, s_2, \dots, s_k)] \rangle_{\hat{\alpha}_w, \alpha_w}, \quad (\text{S43})$$

$$q^l = \sum_{\{\hat{s}_j, s_j\}} \prod_{j=1}^k \left[ \frac{1 + \hat{s}_j \hat{m}^{l-1} + s_j m^{l-1} + \hat{s}_j s_j q^{l-1}}{4} \right] \times \langle \tanh [\beta \hat{\alpha}_w (\hat{s}_1, \hat{s}_2, \dots, \hat{s}_k)] \tanh [\beta \alpha_w (s_1, s_2, \dots, s_k)] \rangle_{\hat{\alpha}_w, \alpha_w}. \quad (\text{S44})$$

In the following we assume  $k$  is odd.

### 1. Average over weight disorder

We consider the weights to be independent quench random variables drawn from the distribution

$$P_w(\hat{w}_{ij}^l) = \delta_{\hat{w}_{ij}^l, 1}, \quad (\text{S45})$$

$$\begin{aligned} P_w(w_{ij}^l) &= (1-p)\delta_{w_{ij}^l, \hat{w}_{ij}^l} + p\delta_{w_{ij}^l, -\hat{w}_{ij}^l} \\ &= (1-p)\delta_{w_{ij}^l, 1} + p\delta_{w_{ij}^l, -1}. \end{aligned} \quad (\text{S46})$$

In the limit  $\beta \rightarrow \infty$ , we have  $\tanh [\beta \alpha_w (s_1, s_2, \dots, s_k)] = \text{sgn} \left( \sum_{j=1}^k w_j s_j \right)$  where  $w_j$  follows the distribution  $P_w(w_j)$  in Eq. (S46). Including the disorder distributions Eq. (S45) and Eq. (S46) in the saddle point equations gives

$$m^l = \sum_{\{s_j\}} \prod_{j=1}^k \left[ \frac{1 + s_j m^{l-1}}{2} \right] \sum_{\{w_j\}} P_w(\{w_j\}) \text{sgn} \left( \sum_{j=1}^k w_j s_j \right), \quad (\text{S47})$$

$$q^l = \sum_{\{\hat{s}_j, s_j\}} \prod_{j=1}^k \left[ \frac{1 + \hat{s}_j \hat{m}^{l-1} + s_j m^{l-1} + \hat{s}_j s_j q^{l-1}}{4} \right] \text{sgn} \left( \sum_{j=1}^k \hat{s}_j \right) \sum_{\{w_j\}} P_w(\{w_j\}) \text{sgn} \left( \sum_{j=1}^k w_j s_j \right). \quad (\text{S48})$$

These expressions can be further simplified as follows. We start with Eq. (S43) by defining a new spin variable  $\sigma_j := w_j s_j$ , through the integral representation of the Kronecker delta

$$\delta(\sigma_j, w_j s_j) = \int_{-\pi}^{\pi} \frac{d\theta_j}{2\pi} e^{i\theta_j(\sigma_j - w_j s_j)} = \begin{cases} 1 & \text{if } \sigma_j = w_j s_j \\ 0 & \text{others} \end{cases} \quad (\text{S49})$$

$$\sum_{\sigma_j = \pm 1} \delta(\sigma_j, w_j s_j) = 1. \quad (\text{S50})$$

It allows us to express the dynamics of the magnetization as

$$\begin{aligned} m^l &= \sum_{\{s_j\}} \prod_{j=1}^k \left[ \frac{1 + s_j m^{l-1}}{2} \right] \sum_{\{w_j\}} P(\{w_j\}) \sum_{\{\sigma_j\}} \prod_j \delta(\sigma_j, w_j s_j) \text{sgn} \left( \sum_{j=1}^k w_j s_j \right) \\ &= \sum_{\{s_j\}} \prod_{j=1}^k \left[ \frac{1 + s_j m^{l-1}}{2} \right] \sum_{\{w_j\}} P(\{w_j\}) \sum_{\{\sigma_j\}} \prod_j \int_{-\pi}^{\pi} \frac{d\theta_j}{2\pi} e^{i\theta_j(\sigma_j - w_j s_j)} \text{sgn} \left( \sum_{j=1}^k \sigma_j \right). \end{aligned} \quad (\text{S51})$$

We then notice that

$$\begin{aligned} &\sum_{\{w_j\}} P(\{w_j\}) e^{-i \sum_{j=1}^k \theta_j w_j s_j} \\ &= \sum_{\{w_j\}} \prod_j \{ [p\delta_{w_j, -1} + (1-p)\delta_{w_j, 1}] e^{-i\theta_j w_j s_j} \} \\ &= \prod_j [p e^{i\theta_j s_j} + (1-p)e^{-i\theta_j s_j}], \end{aligned} \quad (\text{S52})$$



which leads to

$$\begin{aligned}
m^l &= \sum_{\{\sigma_j\}} \sum_{\{s_j\}} \prod_{j=1}^k \left\{ \left[ \frac{1+s_j m^{l-1}}{2} \right] \int_{-\pi}^{\pi} \frac{d\theta_j}{2\pi} e^{i\theta_j \sigma_j} [p e^{i\theta_j s_j} + (1-p) e^{-i\theta_j s_j}] \right\} \text{sgn} \left( \sum_{j=1}^k \sigma_j \right) \\
&= \sum_{\{\sigma_j\}} \sum_{\{s_j\}} \prod_{j=1}^k \left\{ \left[ \frac{1+s_j m^{l-1}}{2} \right] [p \delta(s_j, -\sigma_j) + (1-p) \delta(s_j, \sigma_j)] \right\} \text{sgn} \left( \sum_{j=1}^k \sigma_j \right) \\
&= \sum_{\{s_j\}} \prod_{j=1}^k \left[ \frac{1+s_j m^{l-1}(1-2p)}{2} \right] \text{sgn} \left( \sum_{j=1}^k s_j \right), \tag{S53}
\end{aligned}$$

where in the last step we trace over  $\{\sigma_j\}$  and replace the dummy spin variables  $\{\sigma_j\}$  by  $\{s_j\}$ .

Performing the same derivation for the dynamics of the overlap in Eq. (S48), we have

$$\begin{aligned}
q^l &= \sum_{\{\hat{s}_j, s_j\}} \prod_{j=1}^k \left[ \frac{1 + \hat{s}_j \hat{m}^{l-1} + s_j m^{l-1} + \hat{s}_j s_j q^{l-1}}{4} \right] \text{sgn} \left( \sum_{j=1}^k \hat{s}_j \right) \sum_{\{w_j\}} P(w_j) \sum_{\{\sigma_j\}} \prod_j \delta(\sigma_j, w_j s_j) \text{sgn} \left( \sum_{j=1}^k \sigma_j \right) \\
&= \sum_{\{\hat{s}_j, s_j\}} \prod_{j=1}^k \left[ \frac{1 + \hat{s}_j \hat{m}^{l-1} + s_j m^{l-1} + \hat{s}_j s_j q^{l-1}}{4} \right] \text{sgn} \left( \sum_{j=1}^k \hat{s}_j \right) \sum_{\{\sigma_j\}} \prod_j [p \delta(s_j, -\sigma_j) + (1-p) \delta(s_j, \sigma_j)] \text{sgn} \left( \sum_{j=1}^k \sigma_j \right) \\
&= \sum_{\{\hat{s}_j, s_j\}} \prod_{j=1}^k \left[ \frac{1 + \hat{s}_j \hat{m}^{l-1} + s_j m^{l-1}(1-2p) + \hat{s}_j s_j q^{l-1}(1-2p)}{4} \right] \text{sgn} \left( \sum_{j=1}^k \hat{s}_j \right) \text{sgn} \left( \sum_{j=1}^k s_j \right), \tag{S54}
\end{aligned}$$

where in the last step we trace again over  $\{\sigma_j\}$  and replace the dummy spin variables  $\{\sigma_j\}$  by  $\{s_j\}$ .

## 2. Expressions for $k = 3$

For the particular case of  $k = 3$ , we have equations of the form

$$\hat{m}^l = \frac{1}{2} [3\hat{m}^{l-1} - (\hat{m}^{l-1})^3], \tag{S55}$$

$$m^l = \frac{1}{2} [3m^{l-1}(1-2p) - (m^{l-1})^3(1-2p)^3], \tag{S56}$$

$$\begin{aligned}
q^l &= \frac{3}{2} \hat{m}^{l-1} m^{l-1} (1-2p) - \frac{3}{4} q^{l-1} (m^{l-1})^2 (1-2p)^3 - \frac{3}{4} q^{l-1} (\hat{m}^{l-1})^2 (1-2p) \\
&\quad + \frac{3}{4} q^{l-1} (1-2p) + \frac{1}{4} (q^{l-1})^3 (1-2p)^3. \tag{S57}
\end{aligned}$$

The evolutions of  $m^l$  and  $q^l$  are validated by Monte Carlo simulations as shown in Fig. S4.

In the deep network limit  $l \rightarrow \infty$ ,  $m^\infty = 0$  is always a solution of Eq. (S56), which is stable for  $p > p_c = 1/6$ . For  $p < 1/6$ , the solution  $m^\infty = 0$  becomes unstable and two stable solutions emerge  $m^\infty = \pm \sqrt{\frac{1-6p}{(1-2p)^3}}$ .

Consider the initial condition  $\hat{m}^0 = m^0 > 0$  and  $q^0 = 1$ , then the reference function admits a stationary solution  $\hat{m}^\infty = 1$ , which implies  $\hat{s}_i^\infty = 1, \forall i$ . So we have the relation  $q^\infty = \frac{1}{N} \sum_i \hat{s}_i^\infty s_i^\infty = \frac{1}{N} \sum_i s_i^\infty = m^\infty$ .

## 3. Critical Perturbation $p_c$ for general $k$

By examining the stability of the steady solution  $m^\infty = 0$  in Eq. (S53), we can derive the the critical perturbation  $p_c$  for general  $k$ . We first notice that Eq. (S53) can be expressed as

$$m^l = \sum_{n=0}^k \binom{k}{n} \left[ \frac{1+m^{l-1}(1-2p)}{2} \right]^n \left[ \frac{1-m^{l-1}(1-2p)}{2} \right]^{k-n} \text{sgn}(2n-k). \tag{S58}$$

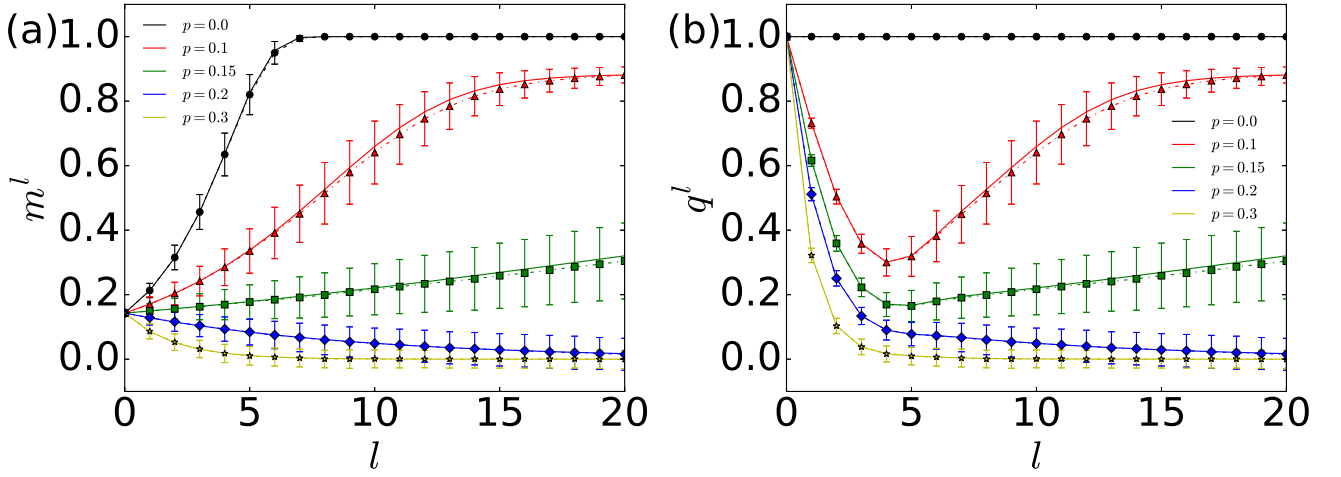


Figure S4. Comparing the mean field order parameter evolution in layers following Eq. (S56) in (a) and Eq. (S57) in (b) (solid lines) to Monte Carlo simulations (dashed-dotted lines with markers). The results show a perfect match between analysis and numerical results. The systems are of size  $N = 2000$  and the results are averaged over 100 disorder realizations.

Perturbing  $m^{l-1}$  and  $m^l$  around 0 gives

$$\delta m^l = \sum_{n=0}^k \binom{k}{n} \left\{ (k-n) \left(\frac{1}{2}\right)^{k-1} \left(-\frac{1-2p}{2} \delta m^{l-1}\right) + n \left(\frac{1}{2}\right)^{k-1} \left(\frac{1-2p}{2} \delta m^{l-1}\right) \right\} \text{sgn}(2n-k) + \mathcal{O}((\delta m^{l-1})^2) \quad (\text{S59})$$

$$= \delta m^{l-1} (1-2p) \left(\frac{1}{2}\right)^k \sum_{n=0}^k \binom{k}{n} (2n-k) \text{sgn}(2n-k) + \mathcal{O}((\delta m^{l-1})^2). \quad (\text{S60})$$

By using the identity  $\sum_{n=0}^k \binom{k}{n} (2n-k) \text{sgn}(2n-k) = 2k \binom{k-1}{(k-1)/2}$  for odd integer  $k$ , one obtains the instability condition

$$\frac{\delta m^l}{\delta m^{l-1}} = (1-2p) \left(\frac{1}{2}\right)^{k-1} k \binom{k-1}{(k-1)/2} > 1, \quad (\text{S61})$$

$$p < p_c(k) := \frac{1}{2} - 2^{k-2} / \left[ k \binom{k-1}{(k-1)/2} \right]. \quad (\text{S62})$$

The obtained critical flip noise  $p_c(k)$  in Eq. (S62) has exactly the same form as the critical thermal noise  $\epsilon_c(k)$  [S4]. Therefore, they show the same locations for the corresponding phase transitions.

\* bliaf@connect.ust.hk

† d.saad@aston.ac.uk

[S1] C. De Dominicis, Phys. Rev. B **18**, 4913 (1978).

[S2] H. S. Seung, H. Sompolinsky, and N. Tishby, Phys. Rev. A **45**, 6056 (1992).

[S3] A. Engel and C. V. d. Broeck, *Statistical Mechanics of Learning* (Cambridge University Press, New York, 2001).

[S4] A. Mozeika, D. Saad, and J. Raymond, Phys. Rev. E **82**, 041112 (2010).